Information diversity and anomalous scaling in asymmetric social contagion process on low-dimensional static networks

Kwanwoo Kim and Soon-Hyung Yook*
Department of Physics and Research Institute for Basic Sciences, Kyung Hee University, Seoul 02447, Korea

(Received 10 October 2022; accepted 1 March 2023; published 15 March 2023)

To understand how competition affects the diversity of information, we study the social contagion model introduced by Halvorsen-Pedersen-Sneppen (HPS) [G. S. Halvorsen, B. N. Pedersen, and K. Sneppen, Phys. Rev. E **103**, 022303 (2021)] on one-dimensional (1D) and two-dimensional (2D) static networks. By mapping the information value to the height of the interface, we find that the width $W(N,t)$ does not satisfy the well-known Family-Vicsek finite-size scaling ansatz. From the numerical simulations, we find that the dynamic exponent z should be modified for the HPS model. For 1D static networks, the numerical results show that the information landscape is always rough with an anomalously large growth exponent, β. Based on the analytic derivation of $W(N,t)$, we show that the constant small number of influencers created for unit time and the recruitment of new followers are two processes responsible for the anomalous values of β and z. Furthermore, we also find that the information landscape on 2D static networks undergoes a roughening transition, and the metastable state emerges only in the vicinity of the transition threshold.

DOI: 10.1103/PhysRevE.107.034307

I. INTRODUCTION

The spread of information such as news, ideas, cultural traits, or new technology on a social network takes place through social contagion processes [1–7]. In traditional models for information dissemination, the mass media has played the role of the outlet of news or new information. The nontrivial effect of mass media on cultural dissemination has been investigated [8–10]. In contrast to the traditional models, due to the recent explosive growth of online social network services, each individual now plays the roles of the news provider and the news consumer. Furthermore, some members of such global online social networks collect a huge number of followers through social interactions and become an influencer.

In such information-spreading dynamics on social networks, competition is ubiquitous and is known to cause nontrivial phenomena [11,12]. Recently, Halvorsen-Pedersen-Sneppen (HPS) introduced a simple model to investigate how influencers compete for attention on an asymmetric social network [13]. In the HPS model, the global asymmetric interactions between influencers and followers are integrated into local reciprocal interactions. The local reciprocal interactions are represented by the static undirected network. The basic idea of the HPS model is that the influencers build up a network of followers through interaction along the local reciprocal network. The capacity for interaction is determined by the age of the information [13]. It means that the users are more attracted to the new information than to the old information. The novelty of information is known to cause many interesting phenomena in information dynamics, such as the evolution of popularity [14–17]. The probability to produce new information in the HPS model is proportional to the degree of the node (or the number of followers) in the global asymmetric network. The degree-dependent probability of the HPS model causes a nontrivial phase transition as in the opinion dynamics model [18]. In addition, the HPS model assumes that each follower maintains only one directed link to an influencer which represents limited attention [19]. This limited attention causes local competition between information.

From the numerical simulations, Halvorsen *et al.* found that the HPS model shows many interesting phenomena due to the competition for attention among the information providers on social networks [13]. For example, by measuring the time-averaged size of the largest subculture on finite networks, they suggested that there can be a phase transition from a highly ordered regime to a disordered regime of a multicultural state. In addition, they also showed that there is a metastable state in which one influencer maintains dominance for a sustained period. This metastable state decays into a fragmented state that divides attention between influencers or jumps to another metastable state. Even in the highly ordered regime, they addressed that the jumps between different metastable states were possibly observed.

In this paper, we investigate the dynamical properties of the information diversity generated by the HPS model. For this, we map the value of the information into the height of the interface as in the innovation spreading model [3,4], and we analyze the numerical results with the finite-size scaling (FSS) ansatz. Although social interaction networks can have long-range connections and heterogeneous topology [20,21], we restrict ourselves to low-dimensional cases, leaving the analysis of such heterogeneous structures for the future. By carefully redefining the control parameters and measuring the width of the information landscape, we find that the width

*syook@khu.ac.kr

of the information landscape shows an anomalous scaling behavior. Furthermore, we find that the HPS model is always in the fragmented rough phase for one-dimensional (1D) static social networks. On the other hand, the model undergoes a roughening transition on two-dimensional (2D) static social networks as we change the control parameters. We also find that the metastable state emerges only in the vicinity of the transition threshold on 2D static networks.

This paper is organized as follows. In Sec. II the definition of the model is provided. The numerical results and analytical derivations on both 1D and 2D static networks are in Sec. III. In Sec. IV we summarize our results.

II. MODEL

The HPS model on the low-dimensional regular lattice is defined as follows [13]. Let N be the number of nodes communicating through the d-dimensional static social connections. Each node i is characterized by the state $\phi_i = F$ or I. Here F represents a follower state and I denotes an influencer state, respectively. Each node i also has information whose value is τ_i. Let $p_i = p_0(1 + \eta k_i)$ be the probability that a node i generates new information. Here k_i is the number of followers of node i and η is a positive feedback parameter between information creation and the number of followers. Thus, $\{k_i : i = 1, \ldots, N\}$ describes the topology of the influencer-follower network. $k_i = 0$ implies that $\phi_i = F$. Because of the limited attention, each follower is allowed to have at most one directed link to an influencer at any time t. At each unit time step, there are N updates of the state or topology of the influencer-follower network. The influencer-follower network is a time-dependent and directed network.

At $t = 0$ all nodes are in the F state with $\tau = 0$. Let Γ_i be the set of followers of node i. The update rule is defined as follows (see Fig. 1 for schematic illustration).

(i) Randomly select a node i. The chosen node creates new information with a probability p_i. If $\phi_i = F$, then ϕ_i changes from F to I and sets the information value as $\tau_i = t$. On the other hand, if $\phi_i = I$, then it updates its information to $\tau_i = t$, and all its followers also update their information, i.e., $\tau_j = t$ for $\forall j \in \Gamma_i$. With a probability of $1 - p_i$, nothing happens.

(ii) Among the connected neighbors of i along the static social network, we randomly choose a node n. If $\phi_n = F$ and $\tau_i > \tau_n$, then n updates its information value to $\tau_n = \tau_i$. And n disconnects the directed link to the present influencer and follows the same influencer as i. On the other hand, if $\phi_n = I$ and $\tau_i > \tau_n$, then we set $\tau_n = \tau_i$ and $\tau_j = \tau_i$ for $\forall j \in \Gamma_n$.

(iii) To prevent the system from freezing up with influencers who cannot recruit followers, at the end of each time step, all influencers i with $|\Gamma_i| = 0$ change their states $\phi_i = I \to F$. As addressed in Ref. [13], due to the demotion, the number of influencers is eventually saturated around some steady-state value.

The transition between the ordered phase and the disordered phase on 2D static networks is reported in Ref. [13]. From the numerical simulations, they obtained a phase diagram using two control parameters, p_0 and η. However, we find that as $N \to \infty$ the system is always in the ordered state regardless of the value of p_0 for all possible values of η ($\in [0, 1]$) on 2D static networks when we use p_0 as one of the control parameters. It originates from the low information creation rate for $N \gg 1$. As addressed in Ref. [13], p_0 should be sufficiently small to guarantee that p_i never exceeds unity. When $p_0 \ll 1$ an emerging influencer recruits most of the nodes as its followers before the next information creation event occurs. In order to avoid the effect of a low-information creation rate on the possible phase transition, we use Np_0 as the control parameter instead of p_0. Here Np_0 is the lower bound of the average number of information created for a unit time interval. We also restrict the range of p_0 to $p_0 \in [0, 1/N]$ as in Ref. [13]. As we shall show, this modification of the control parameter gives a robust phase diagram.

III. WIDTH AND FAMILY-VICSEK FSS ANSATZ

In order to measure the diversity of information value, we use the concepts developed in the studies on kinetic surface roughening [22]. To do this, we map the information value of each node into the height of the interface. The roughness of the interface (or the information diversity) is generally described by the width $W(N, t)$, defined as

$$W(N, t) \equiv \left(\frac{1}{N} \sum_{i=1}^{N} [\tau_i(t) - \bar{\tau}(t)]^2 \right)^{1/2}. \tag{1}$$

Here, $\bar{\tau}(t)$ represents the average information value at time t,

$$\bar{\tau}(t) \equiv \frac{1}{N} \sum_{i=1}^{N} \tau_i(t). \tag{2}$$

When the interface is self-affine, $W(N, t)$ is known to satisfy the Family-Vicsek FSS ansatz [23]:

$$W(N, t) \sim N^{\alpha} f\left(\frac{t}{N^z} \right), \tag{3}$$

where the function $f(x)$ scales as $f(x) \sim x^{\beta}$ for $x \ll 1$ and $f(x) \to$ const. for $x \gg 1$. The dynamic exponent z satisfies the relation $z = \alpha/\beta$. Here, since the information can also spread along the influencer-follower network, we use the number of nodes N instead of the linear dimension L of the static underlying networks in Eq. (3).

IV. RESULTS

A. Numerical results on 1D static networks

As the simplest case, we first study the behavior of $W(N, t)$ on 1D static networks. In Fig. 2(a) we show the obtained $W(N, t)$'s for $N = 2048 \sim 16\,384$ on 1D static networks with $(Np_0, \eta) = (1.0, 0.5)$. As expected from Eq. (3), we find that $W(N, t)$ grows as

$$W(N, t) \sim t^{\beta} \tag{4}$$

for the initial transient period. From the best fit of Eq. (4) to the data, we obtain $\beta = 1.9 \pm 0.1$ for $N = 16\,384$. This initial growing regime is followed by a saturated regime at which $W(N, t \to \infty) = W_{\text{sat}}(N)$. From Eq. (3), we expect that $W_{\text{sat}}(N)$ satisfies the scaling relation

$$W_{\text{sat}}(N) \sim N^{\alpha}. \tag{5}$$

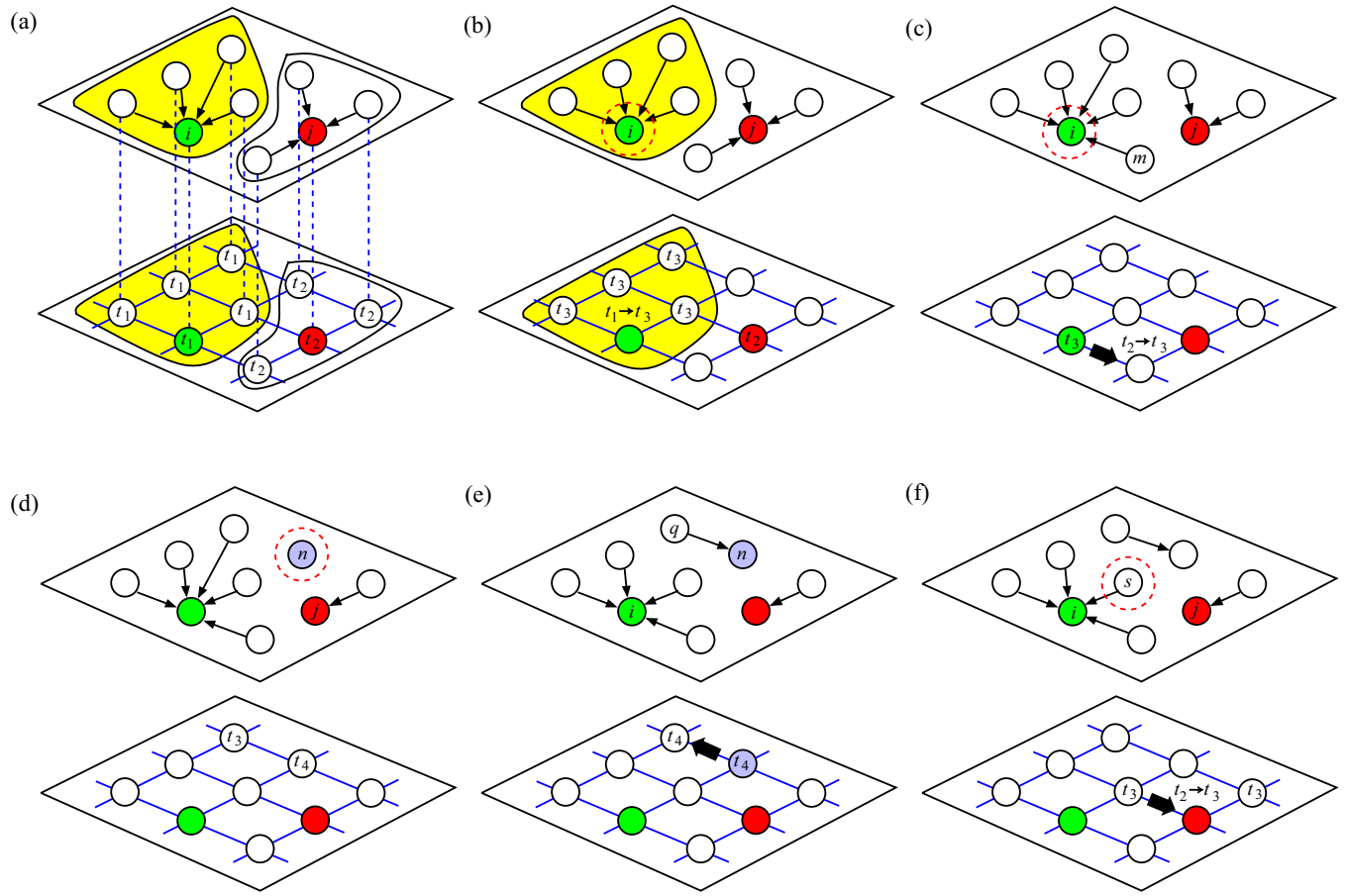

FIG. 1. Schematic illustration of the HPS model on a two-dimensional static network. The upper layers represent the influencer-follower (or global asymmetric) networks and the lower layer denotes the two-dimensional static social connection (or local reciprocal interactions). Solid circles are the influencers and the open circles are the followers. Arrows in the upper layers stand for influencer-follower relations. We assume $t_i < t_{i+1}$ $(i = 2, 3, \ldots)$. (a) There are initially two different information clusters. Each cluster is enclosed by a closed path. The node i (j) is an influencer with $\tau_i = t_1$ $(\tau_j = t_2)$. The dashed lines between the layers denote that the two nodes connected by the dashed line are the same. (b) At $t = t_3$, the node i (marked by the dashed circle) is randomly selected and creates new information $(\tau_i = t_3)$ with a probability p_i. (c) The nearest neighbor of i recruits a follower (node m) among its nearest neighbors in the static network. Since $t_3 > t_2$, m changes its information to $\tau_m = t_3$, disconnects the directed link to j, and makes a new link to i. The thick arrow in the lower layer denotes the direction of the information flow. (d) At $t = t_4$, the node n is randomly selected and becomes a new influencer by creating new information of $\tau_n = t_4$ with the probability p_n. Thus, n disconnects the directed link to j. (e) The new influencer n recruits its nearest neighbor q as its follower. Thus, the information flows form node n to q. (f) At $t = t_5$, the node s is randomly selected without the creation of new information and selects j to recruit as a follower of i. Let us assume that $t_2 < t_3$. Since the node j is an influencer, j only adopts the information of s $(\tau_j \to t_3)$ without the change of the influencer-follower network.

As shown in the inset of Fig. 2(a), we obtain $\alpha = 0.49 \pm 0.01$. From the obtained α and β we find $z = 0.25 \pm 0.02$. However, as shown in Fig. 2(b), $W(N,t)/N^{\alpha}$ does not collapse into a single curve with the obtained exponents. We find a systematical deviation of $W(N,t)/N^{\alpha}$ for the initial transient regime. This indicates that $W(N,t)$ obtained from the HPS model does not satisfy the Family-Vicsek FSS ansatz (3).

To find the correct scaling form, we measure the crossover time $t_{\times}$ at which $W(N,t)$ crosses over from the behavior of Eq. (4) to that of Eq. (5) for various N. As shown in the inset of Fig. 2(b), we find that $t_{\times}$ scales as

$$t_{\times} \sim N^{z'}, \tag{6}$$

with the modified dynamic exponent $z'(\neq z)$. Using the least-squares fit we obtain $z' = 0.50 \pm 0.02$. Since $W(N,t)$ satisfies Eqs. (4) and (5) [see Fig. 2(a)], only the dynamic exponent z in Eq. (3) is replaced by z'. Thus, we assume that the value of z' should be

$$z' = z + \frac{1}{4} = \frac{\alpha}{\beta} + \frac{1}{2\beta} = \frac{\alpha + \frac{1}{2}}{\beta}. \tag{7}$$

Using these exponents, we modify the FSS ansatz as

$$W(N,t)N^{1/2} \sim N^{\alpha'} f\left(\frac{t}{N^{z'}}\right), \tag{8}$$

where $\alpha' = \alpha + \frac{1}{2}$ and the new dynamic exponent $z' = \alpha'/\beta$. The function $f(x)$ scales as $f(x) \sim x^{\beta}$ for $x \ll 1$ and $f(x) \to$ const. for $x \gg 1$, as in Eq. (3).

In Fig. 3 we replot $W(N,t)$ in the form suggested by Eq. (8) for various values of Np_0 and η. When $\eta = 0$ (without

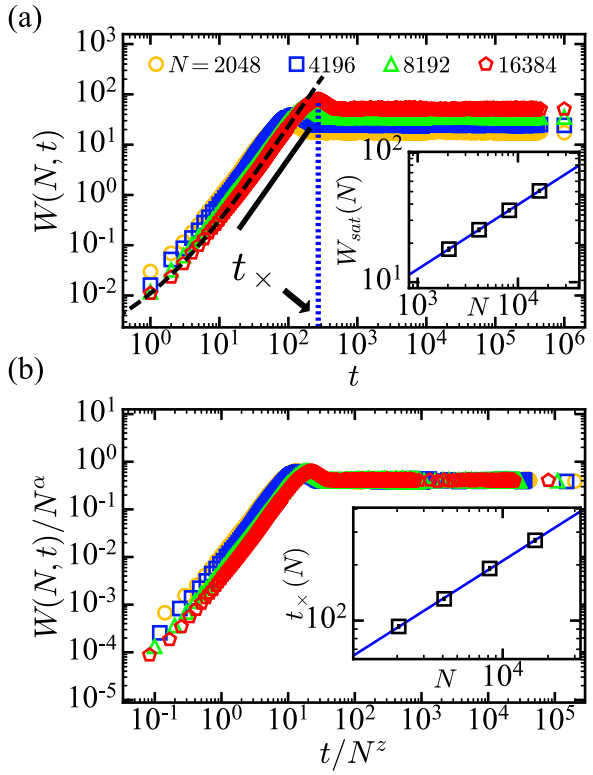

FIG. 2. (a) Plot of $W(N,t)$'s for $N = 2048 \sim 16\,384$ on 1D static networks with $(Np_0, \eta) = (1.0, 0.5)$. $t_\times$ indicates the crossover time for $N = 16\,384$. The solid line represents $W(t) \sim t^{1.94}$. The dashed line denotes Eq. (13). Inset: Plot of $W_{\rm sat}(N)$ against N. The solid line stands for $W_{\rm sat}(N) \sim N^{0.5}$. (b) Scaling plot of $W(N,t)$ using Eq. (3). Inset: Plot of $t_\times(N)$ against N. The solid line represents the relation $t_\times \sim t^{0.5}$.

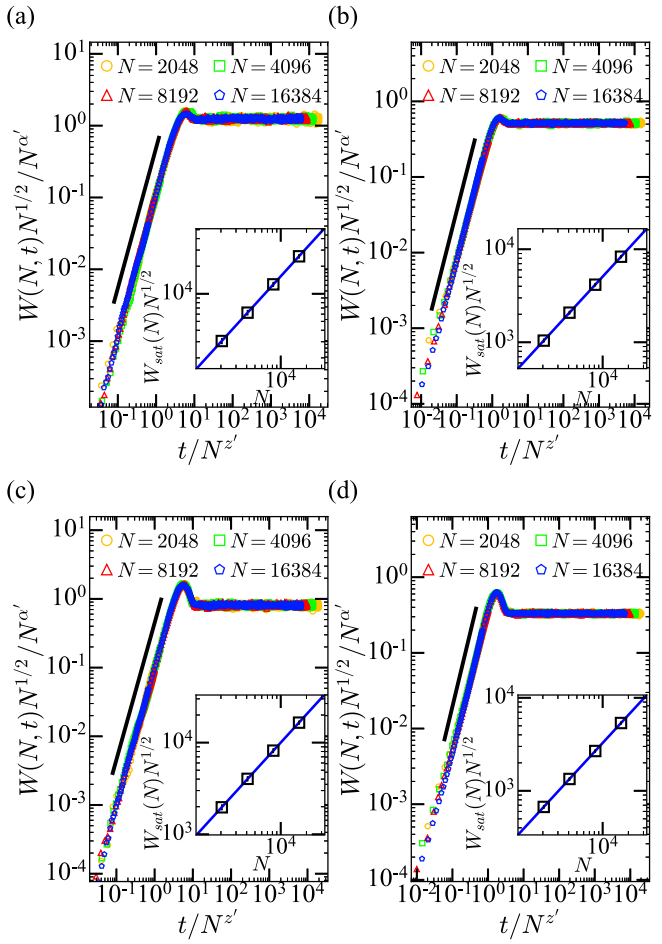

FIG. 3. Scaling collapse of $W(N,t)N^{1/2}$ for (a) $(Np_0, \eta) = (0.1, 0.0)$, (b) $(Np_0, \eta) = (1.0, 0.0)$, (c) $(Np_0, \eta) = (0.1, 1.0)$, and (d) $(Np_0, \eta) = (1.0, 1.0)$. The solid lines represent the relation $W(N,t) \sim t^\beta$ with (a) $\beta \simeq 1.95$, (b) $\beta \simeq 1.85$, (c) $\beta \simeq 1.99$, and (d) $\beta \simeq 1.95$. Insets: Plot of $W_{\rm sat}(N)N^{1/2}$ against N. The solid lines denote the relation $W_{\rm sat}(N) \sim N^{\alpha'}$ with (a) $\alpha' \simeq 1.02$, (b) $\alpha' \simeq 0.99$, (c) $\alpha' \simeq 1.02$, and (d) $\alpha' \simeq 0.99$.

feedback), each node has the same probability, $p_i = p_0$, to create new information and become an influencer, regardless of the value of Np_0. As a result, the information landscape becomes rough for $\eta = 0$. By using Eq. (8), we obtain $\beta = 1.9 \pm 0.1$ for $(Np_0, \eta) = (0.1, 0.0)$ and $\beta = 1.8 \pm 0.2$ for $(Np_0, \eta) = (1.0, 0.0)$ as shown in Figs. 3(a) and 3(b), respectively. From the data in the inset of Figs. 3(a) and 3(b), we find that $W_{\rm sat}(N)N^{1/2}$ satisfies the power law

$$W_{\rm sat}(N)N^{1/2} \sim N^{\alpha'}. \tag{9}$$

From the best fit of Eq. (9) to the data, we obtain $\alpha' = 1.02 \pm 0.02$ for $(Np_0, \eta) = (0.1, 0.0)$ and $\alpha' = 1.00 \pm 0.01$ for $(Np_0, \eta) = (1.0, 0.0)$. Using the obtained values of α' and β, we estimate the dynamic exponent $z' = 0.53 \pm 0.03$ for $(Np_0, \eta) = (0.1, 0.0)$ and $z' = 0.55 \pm 0.07$ for $(Np_0, \eta) = (1.0, 0.0)$. As shown in Figs. 3(a) and 3(b), $W(N,t)N^{1/2}$ shows a good scaling collapse with these exponents, confirming the suggested modified FSS ansatz (8). For other values of (Np_0, η), we find the same scaling behavior with identical exponents within the estimated error [see Figs. 3(c) and 3(d)]. The obtained exponents are $\beta = 2.0 \pm 0.3$ and $\alpha' = 1.0 \pm 0.1$, for all possible values of (Np_0, η). These results clearly show that the HPS model is always in the rough phase on 1D static networks which is characterized by $\alpha = \alpha' - 1/2 > 0$ [22]. This result coincides with van Hove's nonexistence theorem [24] as addressed in Ref. [13].

B. Analytic derivation of the exponents for 1D static networks

The value of β in many interface growth models is generally smaller than 1 [22]. However, we obtain $\beta \approx 2$ in the HPS model on the 1D static network. In order to understand the anomalously large value of β, we focus on two processes for the initial growth of the information value: (i) The constant and small number of influencers which is created for a unit time interval and (ii) the recruitment of followers. For the initial transient period, process (i) means that there is at most one node which can create new information and become an influencer at each time step, since $p_0 \leqslant 1/N$. By the definition of the model, the value of information of the influencer is given by the time at which the node becomes the influencer. This value of information is also hardly changed for the initial period due to the small value of p_0 for $N \gg 1$. Furthermore, the total number of influencers during this period is very small

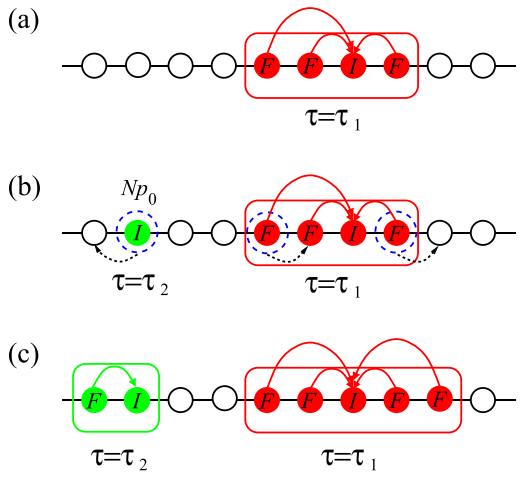

FIG. 4. Schematic diagram for the early-time evolution of clusters on the 1D static network at $t = \tau_2$ ($\tau_2 > \tau_1$). (a) The (red) rectangle denotes the cluster of nodes following the same influencer whose information value is τ_1. The solid arrows on the top of nodes denote the follower network. The (white) open circles are nodes of $\tau = 0$ whose state is $\phi = F$, but they do not follow any influencer. (b) A node (green circle) creates new information at $t = \tau_2$ with a probability p_0 and becomes an influencer. The (blue) dashed circles are the nodes at the boundary of each cluster. Each boundary node randomly selects one of its neighbors on a static network [represented by (black) dotted arrows]. (c) The node at the right boundary of the cluster of τ_1 recruits a new follower and $s_{\tau_1} = 5$, while the node at the left boundary cannot recruit a new node because it selects the node in the same cluster. At the same time, the new influencer recruits one of its neighbors and $s_{\tau_2}(\tau_2) = 2$.

compared to N and sparsely distributed over the 1D static network.

Let $s_\tau(t)$ be the size of the cluster τ at t ($t \geqslant \tau$). $s_\tau(t)$ is composed of an influencer whose information value is τ and its $k_\tau (= s_\tau - 1)$ followers. The nodes in the cluster share the same information created at τ. The schematic diagram for the evolution of clusters is depicted in Fig. 4. When a node becomes an influencer, it also recruits one of its nearest neighbors in the static network as its follower. Thus, $s_\tau(\tau) = 2$. For $t > \tau$, the influencer created at τ can only recruit followers due to the low information creation rate. Since only the nodes located at the boundary of the cluster can recruit followers [see Fig. 4(b)], the time evolution of $s_\tau(t)$ can be written as

$$s_\tau(t) = 2 + c(t - \tau). \tag{10}$$

Here $c = 1$ for the 1D static network (see Fig. 4) because the cluster whose size is larger than two recruits one neighboring node at each t on average.

Let us consider the case $Np_0 = 1$ for simplicity. Then, only one node changes its state to I on average at each time step. Thus, at t there are t influencers in the network when $t \ll t_\times$. The total number of nodes with $\tau > 0$, $K(t)$, is

$$K(t) = \sum_{\tau=1}^{t} s_\tau(t). \tag{11}$$

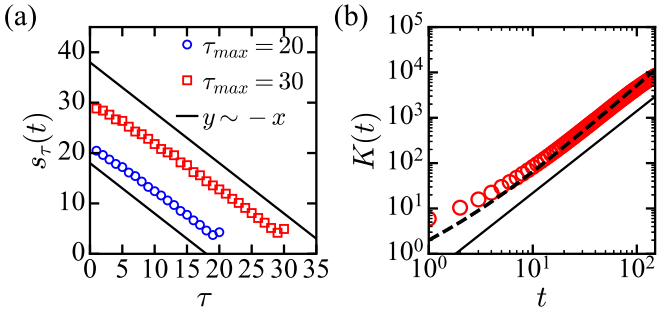

FIG. 5. (a) Plot of $s_\tau(t)$'s against τ for $Np_0 = 1.0$, $\eta = 1.0$, and $N = 16\,384$ when $\tau_{\max}$ reaches $\tau_{\max} = 20$ and $\tau_{\max} = 30$. The solid lines represent the relation $s_\tau(t) \sim -\tau$. (b) Plot of $K(t)$ against t. The solid line denotes the relation $K(t) \sim t^\delta$ with $\delta = 1.8$. The dashed line represents Eq. (15).

From Eqs. (1), (10), and (11), we rewrite $W(N, t)$ as

$$W(N,t) = N^{-1/2}\left[\sum_{\tau=1}^{t} s_\tau(t)(\tau - \bar{\tau})^2 + [N - K(t)]\bar{\tau}^2\right]^{1/2}. \tag{12}$$

Since $\bar{\tau} = \sum_{\tau=1}^{t} s_\tau \tau / N \ll 1$ for $N \gg 1$, we ignore $\bar{\tau}$ in Eq. (12). Using Eq. (10), $W(N, t)$ can be approximated as

$$\begin{aligned} W(N,t) &\approx N^{-1/2}\left[\sum_{\tau=1}^{t}[2 + (t - \tau)]\tau^2\right]^{1/2} \\ &\approx N^{-1/2}[t(t+1)(t^2 + 7t + 4)/12]^{1/2}. \end{aligned} \tag{13}$$

In Fig. 2(a) we display Eq. (13) for the initial transient period. As shown in Fig. 2(a), Eq. (13) agrees very well with the numerical result. Therefore, we obtain

$$W(N,t)N^{1/2} \sim t^2 \sim t^\beta, \tag{14}$$

with $\beta = 2$.

Furthermore, we can also obtain z' from Eq. (11). For 1D static networks, Eq. (11) is approximated as

$$K(t) = t(t+3)/2 \sim t^\delta, \tag{15}$$

where $\delta = 2$. At $t \approx t_\times$, $K(t_\times)$ becomes comparable with N. Thus, we find that $t_\times \sim N^{1/2} \sim N^{z'}$ or $z' = 1/2$ for 1D static networks. These values of β and z' give $\alpha' = 1$. By combining Eq. (14) with the behavior of $K(t)$ in the vicinity of $t_\times$, we obtain the modified FSS ansatz, Eq. (8). The exponents obtained analytically agree very well with those obtained from the numerical simulations (see Fig. 3).

To validate our assumption, we measure $s_\tau(t)$ and $K(t)$ from the numerical simulations. Figure 5(a) shows the measured $s_\tau(t)$'s from the numerical simulations for $(Np_0, \eta) = (1.0, 1.0)$, when the maximum value of τ reaches $\tau_{\max} = 20$ and $\tau_{\max} = 30$, respectively. From the data, we find that $s_\tau(t) \sim -\tau$, which shows a good agreement with Eq. (10). We also display the obtained $K(t)$ from the same simulations in Fig. 5(b) and compare it with the analytic expression (15) (dashed line). From the least-squares fit of Eq. (15) to the data, we obtain $\delta = 1.8 \pm 0.2$. This value of δ agrees with the analytic expectation $\delta = 2$ within the estimated error. This analysis can be directly extended to the case of 2D static networks.

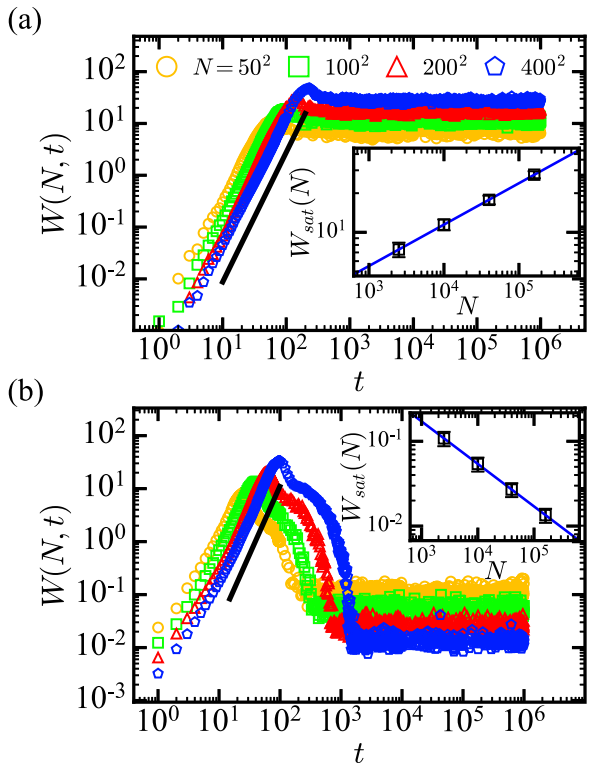

FIG. 6. Plot of $W(N,t)$'s on 2D static networks for (a) $(Np_0, \eta) = (0.1, 0.0)$ and (b) $(Np_0, \eta) = (1.0, 1.0)$. The solid lines represent the relations (a) $W(N,t) \sim t^{2.5}$ and (b) $W(N,t) \sim t^{2.6}$. Insets: Plots of $W_{\rm sat}(N)$'s. The solid lines denote (a) $W_{\rm sat}(N) \sim N^{0.32}$ and (b) $W_{\rm sat}(N) \sim N^{-0.5}$.

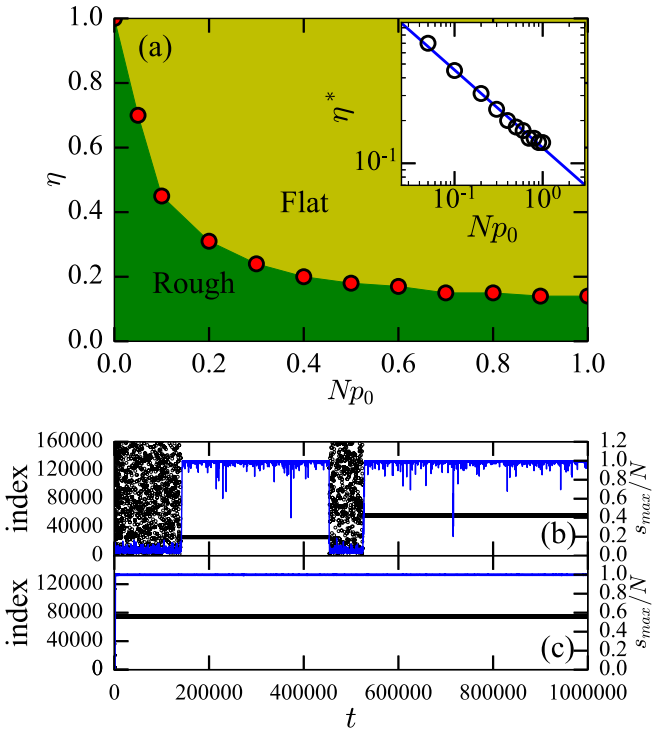

FIG. 7. (a) Phase diagram of the HPS model. Dark green (gray) represents the rough phase and light green (gray) corresponds to the flat phase. Inset: Plot of η^* against Np_0. The solid line represents the relation $\eta^* \sim (Np_0)^{-1/2}$. Black circles in panels (b) and (c) denote the index of the influencer node belonging to the largest cluster at t for (b) $(Np_0, \eta) = (1.0, 0.15)$ and (c) $(Np_0, \eta) = (1.0, 1.0)$. Blue (gray) lines represent the evolution of $s_{\rm max}/N$ for $N = 400 \times 400$.

C. Numerical results on 2D static networks

For 2D static networks, we use the square lattice whose linear dimension is L ($N = L^2$). On 2D static networks, we find that the behavior of $W(N,t)$ strongly depends on Np_0 and η. In Fig. 6 we show two limiting cases of $W(N,t)$ on 2D static networks. In Fig. 6(a) we display $W(N,t)$'s for $(Np_0, \eta) = (0.1, 0.0)$ as an example of the small values of Np_0 and η. When Np_0 and η are small, we find that $W(N,t)$ seems to satisfy the FSS ansatz, Eq. (3) or Eq. (8), as shown in Fig. 6(a). By fitting Eqs. (4) and (5) to the data, we obtain $\beta = 2.5 \pm 0.2$ for $t < t_\times$ and $\alpha = 0.32 \pm 0.01$ when $t > t_\times$.

As an example for large Np_0 and η, we display $W(N,t)$'s for $(Np_0, \eta) = (1.0, 1.0)$ in Fig. 6(b). When Np_0 and η are large, we find that $W(N,t)$ initially grows as $W(N,t) \sim t^\beta$ until competition between clusters arises. At $t \approx t_\times$, small clusters start being merged into large clusters as a result of competition. Thus, $W(N,t)$ decreases and reaches a steady-state value, $W_{\rm sat}(N)$ with $\alpha < 0$. From the least-squares fit of Eq. (4) to the data, we find that $\beta \simeq 2.6$, which is very close to the value of β obtained in Fig. 6(a). Furthermore, as shown in the inset of Fig. 6(b), $W_{\rm sat}(N)$ decreases as N increases. From the data, we obtain $\alpha \simeq -1/2$, which clearly shows that a single influencer dominates for large Np_0 and η. Note that $\alpha < 0$ means that the fluctuation of the information value vanishes in the limit $N \to \infty$. Therefore, the information landscape of the HPS model undergoes a transition from the rough phase to the flat one as we increase Np_0 and η. In Fig. 7(a) we plot the phase diagram for the observed roughening transition. Here the transition threshold (Np_0^*, η^*) is defined as those values at which $\alpha = 0$ or equivalently $\alpha' = 1/2$. The inset of Fig. 7(a) shows that η^* satisfies another power-law relation:

$$\eta^* \sim (Np_0)^{-1/2}. \tag{16}$$

Equation (16) verifies that Np_0 is a better control parameter than p_0. If we use p_0 as a control parameter, then $Np_0 \to \infty$ for a given value of $p_0 (> 0)$ in the limit $N \to \infty$. Thus, $\eta^* \to 0$ by Eq. (16). As a result, we always obtain the flat ordered phase in the thermodynamic limit if we use p_0 as one of the control parameters.

Figure 7(b) shows the influencer index that belongs to the largest cluster at t for $(Np_0, \eta) = (1.0, 0.15)$ and the time evolution of $s_{\rm max}/N$. Here $s_{\rm max}$ is the size of the largest cluster. $(Np_0, \eta) = (1.0, 0.15)$ corresponds to the vicinity of the transition threshold. The data clearly show that there are metastable states where one influencer maintains dominance for a sustained period in the steady state. The first metastable state emerges around $t = 1.5 \times 10^5$ and is sustained to $t \approx 4.5 \times 10^5$. This metastable state collapses into small clusters, causing a sudden drop in $s_{\rm max}/N$, and another metastable state emerges around $t = 5.2 \times 10^5$. Thus, there are jumps between metastable states in the vicinity of the transition threshold, as reported in Ref. [13]. However, in the flat phase, we find

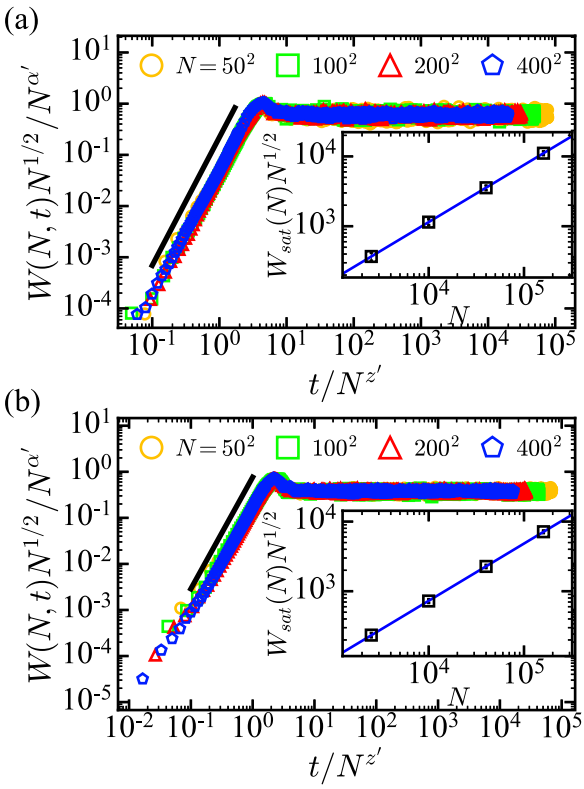

FIG. 8. Scaling collapse of $W(N,t)N^{1/2}$ with $\beta = 2.5$, $\alpha' = 0.82$, and $z' = 0.32$ for (a) $(Np_0, \eta) = (0.1, 0.0)$ and (b) $(Np_0, \eta) = (0.5, 0.1)$.

that such jumps between metastable states are observed only when N is small (which is not shown). As shown in Fig. 7(c), once a node becomes an influencer in the dominant cluster at $t = \tau$, it remains the dominant influencer for $t > \tau$ when N is sufficiently large.

When the information landscape is in the rough phase, we find that $W(N,t)$ satisfies the modified FSS (8). Figure 8 shows the scaling collapse of $W(N,t)$ for $(Np_0, \eta) = (1.0, 0.0)$ and (0.5,0.1) with Eq. (8). Using the least-squares fit, we obtain $\beta = 2.5 \pm 0.2$, $\alpha' = 0.82 \pm 0.01$, and $z' = 0.32 \pm 0.02$ in the rough phase, regardless of (Np_0, η). As shown in Fig. 8, $W(N,t)$'s collapse well into a single curve with the obtained exponents.

D. Analytic derivation of the exponents for 2D static networks

The obtained exponents can also be analytically derived based on the same arguments in Sec. IV B. On 2D static networks, we assume that the cluster following the same influencer is small and compact. Thus, c in Eq. (10) becomes $c \sim t - \tau$, which is proportional to the length of the cluster boundary. Then $s_\tau(t)$ becomes

$$s_\tau(t) \sim (t - \tau)^2. \tag{17}$$

From Eq. (17), the leading order of $W(N,t)$ scales as

$$W(N,t) \sim t^{5/2}. \tag{18}$$

Therefore, we obtain $\beta = 5/2$, which is very close to the value of β obtained from the numerical simulations (see Figs. 6 and 8). Since for $t < t_\times$ the size of the clusters and their information grow in the same fashion for all (Np_0, η), even in the flat phase we obtain the same value of β [see Fig. 6(b)].

From Eq. (17), we rewrite Eq. (11) as

$$K(t) \sim t^3 \tag{19}$$

for 2D static networks. Thus, we expect that $z' = 1/3$ and $\alpha' = 5/6$ in the rough phase on 2D static networks. These values of z' and α' agree very well with those values obtained from the numerical simulations.

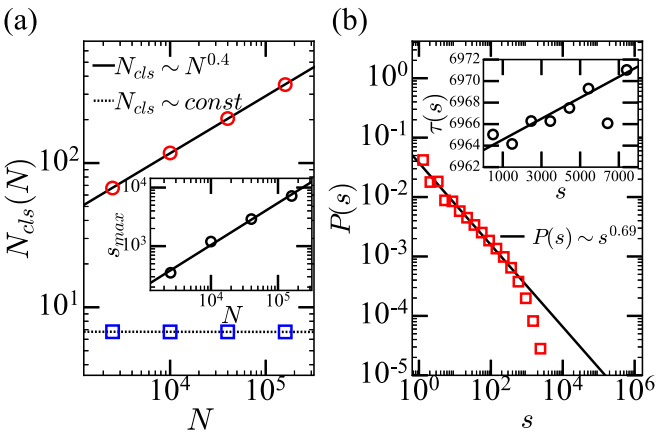

FIG. 9. (a) Plot of $N_{\rm cls}(N)$ against N for $(Np_0, \eta) = (1.0, 1.0)$ (open squares) and $(Np_0, \eta) = (1.0, 0.1)$ (open circles) in the steady state. The dashed line represents $N_{\rm cls} \sim$ const. and the solid line stands for $N_{\rm cls} \sim N^{0.4}$. Inset: Plot of $s_{\rm max}$ against N for $(Np_0, \eta) = (1.0, 0.1)$. The solid line denotes $s_{\rm max} \sim N^{0.72}$. (b) Plot of $P(s)$ for $(Np_0, \eta) = (1.0, 0.1)$. The solid line represents $P(s) \sim s^{0.69}$. Inset: Plot of $\tau(s)$ against s for $N = 400 \times 400$.

E. Properties of clusters on 2D static networks

In Fig. 9(a) we show the number of clusters $N_{\rm cls}$ in the steady state. When the system is in the flat phase [for example, $(Np_0, \eta) = (1.0, 1.0)$], we find that $N_{\rm cls}$ remains at some constant value, $N_{\rm cls} \sim 7$, for all N. Thus, the ratio $N_{\rm cls}/N$ vanishes when $N \to \infty$. In the flat phase, $s_{\rm max}(N)$ becomes $s_{\rm max}(N) \simeq N$ [see, for example, Fig. 7(c)]. This indicates that, even though there is a small number of influencers, only one influencer dominates and most of the nodes follow the same influencer. Therefore, $W_{\rm sat}(N)$ scales as $W_{\rm sat}(N) \sim N^{-1/2}$.

On the other hand, in the rough phase, $N_{\rm cls}$ increases as

$$N_{\rm cls}(N) \sim N^\theta, \tag{20}$$

with $\theta \simeq 0.4$. Note that, even though $N_{\rm cls}$ grows sublinearly or $N_{\rm cls}/N \to 0$ as $N \to \infty$, $W(N,t)$ satisfies the modified FSS (8) with $\alpha > 0$. This can be understood from the nontrivial cluster properties. As shown in the inset of Fig. 9(a), we find that $s_{\rm max}$ in the steady state increases as

$$s_{\rm max} \sim N^\lambda, \tag{21}$$

with $\lambda \simeq 0.7$. In the steady state, the lower-bound of $s_{\rm max}$ approximately satisfies the relation $s_{\rm max} N_{\rm cls} \sim N$. Thus, we expect that $\lambda + \theta \simeq 1$. Furthermore, the cluster size distribution $P(s)$ satisfies a power law in the steady state [see

Fig. 9(b)]:

$$P(s) = Cs^{-\mu}. \tag{22}$$

Here C is a normalization constant. From the least-squares fit of Eq. (22) to the data, we obtain $\mu = 0.7 \pm 0.2$. Since $\mu < 1$, $s_{\max}$ should be finite or grow sublinearly with N to satisfy the normalization condition. Equation (21) and the data in Fig. 9(a) clearly show that $s_{\max}$ grows sublinearly as N increases. Using Eq. (21), we obtain $C \sim N^{-\lambda(1-\mu)}$. As one of the simplest assumptions, let the information value of the cluster of size s, $\tau(s)$, scale as

$$\tau(s) \sim s^{\kappa}. \tag{23}$$

To verify the assumption, we measure $\tau(s)$ from the numerical simulations. As shown in the inset of Fig. 9(b), we find $\tau(s) \sim s$ for $s \gg 1$. Let $n(s)$ be the number of clusters of size s, and then $n(s) = N_{\rm cls}P(s)$. Ignoring the fluctuation of $\tau(s)$ and using the continuum approximation, $\bar{\tau}$ and $\overline{\tau^2}$ in the steady state are approximated as

$$\bar{\tau} \approx \frac{N_{\rm cls}}{N} \int_{s_{\min}}^{s_{\max}} s\tau(s)P(s)ds \tag{24}$$

and

$$\overline{\tau^2} \approx \frac{N_{\rm cls}}{N} \int_{s_{\min}}^{s_{\max}} s\tau^2(s)P(s)ds. \tag{25}$$

From Eqs. (21)–(25), $W(N,t)$ is approximated as

$$W(N,t) = (\overline{\tau^2} - \bar{\tau}^2)^{1/2} \sim N^{[\lambda(2\kappa+1)+\theta-1]/2}, \tag{26}$$

for $t \gg t_{\times}$. Compared to Eq. (9), we obtain the relation

$$2\alpha' = \lambda(2\kappa + 1) + \theta. \tag{27}$$

Equations (26) and (27) indicate that the nontrivial distribution of s can cause the rough phase, which is characterized by $\alpha > 0$.

The values of θ, μ, and κ obtained from the simulations overestimate the value of α'. This discrepancy might originate from the crude approximation in Eqs. (24) and (25) which ignores the fluctuation of $\tau(s)$. However, Eq. (27) quantitatively explains that the nontrivial distribution of s makes the information morphology rough, even though the number of influencers sublinearly grows.

V. SUMMARY

In order to understand how the competition between information affects the diversity of the information, we investigate the HPS model in 1D and 2D static networks by mapping the information value into the height of the interface. Thus, the width $W(N,t)$ quantifies the information diversity. From the numerical simulations on both 1D and 2D static networks, we find that $W(N,t)$ does not satisfy the usual Family-Vicsek FSS ansatz, (3). Furthermore, $W(N,t)$ grows with an anomalously large growth exponent, β, for the initial transient period. From the analytic derivation of $W(N,t)$ we find that the constant and small number of information creation and the recruitment of followers are two main processes responsible for the anomalously large β. The modified dynamic exponent z' can be also obtained from the same argument. The analytically obtained exponents agree very well with the numerical results for 1D and 2D static networks. The analytic derivation, based on these two main processes, also reveals that $W(N,t)$ of the information landscape in the HPS model deviates from the well-known Family-Vicsek FFS ansatz and instead follows the modified FSS ansatz, Eq. (8).

In addition, we find that the information landscape on 1D static networks is always rough, regardless of the value of the control parameters (Np_0, η). However, for 2D static networks, we find that the information landscape undergoes the roughening transition as Np_0 and/or η decreases. From the detailed analysis of the numerical simulations, we also find that the metastable state reported in Ref. [13] emerges only in the vicinity of the transition threshold (Np_0^*, η^*).

As a final remark, the HPS model on complex networks can have practical importance because the topologies of many social interaction networks are suitably described by complex networks. Unlike the low-dimensional cases, there are many dangling ends in the random or scale-free networks. Due to these dangling ends, the boundaries of small clusters which have dangling ends cannot be merged into a large one. The spread of information through the recruiting process is limited by such small clusters having dangling ends. Therefore, we expect that the flattening of the information landscape hardly occurs. The details will be published elsewhere [25].

ACKNOWLEDGMENTS

This work was supported by the National Research Foundation of Korea (NRF) grant funded by the Korean government (MSIT) (Grant No. NRF-2022R1F1A1073629).

[1] R. Axtell, R. Axelrod, J. Epstein, and M. D. Cohen, Comput. Math. Organ. Theory **1**, 123 (1996).
[2] R. Axelrod, J. Conflict Resolut. **41**, 203 (1997).
[3] M. Llas, P. M. Gleiser, J. M. López, and A. Díaz-Guilera, Phys. Rev. E **68**, 066101 (2003).
[4] Y. Kim, B. Han, and S.-H. Yook, Phys. Rev. E **82**, 046110 (2010).
[5] Y. Kim, M. Cho, and S.-H. Yook, Physica A **390**, 3989 (2011).
[6] H. Chae, S.-H. Yook, and Y. Kim, PLoS One **8**, e70928 (2013).
[7] K. Sznajd-Weron and J. Sznajd, Int. J. Mod. Phys. C **11**, 1157 (2000).
[8] Y. Shibanai, S. Yasuno, and I. Ishiguro, J. Conflict Resolut. **45**, 80 (2001).
[9] J. C. González-Avella, M. G. Cosenza, and K. Tucci, Phys. Rev. E **72**, 065102(R) (2005).
[10] J. C. González-Avella, V. M. Eguíluz, M. G. Cosenza, K. Klemm, J. L. Herrera, and M. San Miguel, Phys. Rev. E **73**, 046119 (2006).
[11] J. P. Gleeson, J. A. Ward, K. P. O'Sullivan, and W. T. Lee, Phys. Rev. Lett. **112**, 048701 (2014).

[12] Y. Kim, S. Park, and S.-H. Yook, Sci. Rep. **6**, 23484 (2016).
[13] G. S. Halvorsen, B. N. Pedersen, and K. Sneppen, Phys. Rev. E **103**, 022303 (2021).
[14] S. Asur, B. A. Huberman, G. Szabo, and C. Wang, Trends in social media: Persistence and decay, in *Proceedings of the Fifth International AAAI Conference on Weblogs and Social Media* (2011), Vol. 5, pp. 434–437, https://doi.org/10.1609/icwsm.v5i1.14167.
[15] F. Wu and B. A. Huberman, Proc. Natl. Acad. Sci. USA **104**, 17599 (2007).
[16] S.-H. Yook and Y. Kim, Phys. Rev. E **101**, 012312 (2020).
[17] L. Lizana, M. Rosvall, and K. Sneppen, Phys. Rev. Lett. **104**, 040603 (2010).
[18] M. Kim and S.-H. Yook, Phys. Rev. E **103**, 022302 (2021).
[19] L. Weng, A. Flammini, A. Vespignani, and F. Menczer, Sci. Rep. **2**, 335 (2012).
[20] A.-L. Barabási, *Network Science* (Cambridge University, Cambridge, England, 2016).
[21] M. E. J. Newman, *Networks: An Introduction* (Oxford University, New York, 2010).
[22] A.-L. Barabási and H. E. Stanely, *Fractal Concepts in Surface Growth* (Cambridge University, Cambridge, England, 1995).
[23] F. Family and T. Vicsek, J. Phys. A: Math. Gen. **18**, L75 (1985).
[24] L. van Hove, Physica (Amsterdam) **16**, 137 (1950).
[25] S.-H. Yook and K. Kim (unpublished).